

Tracking Molecular Particles in Live Cells Using Fuzzy Rule-Based System

Shan Jiang,¹ Xiaobo Zhou,^{1,2*} Tom Kirchhausen,³ Stephen T. C. Wong^{1,2}

¹HCNR-Center for Bioinformatics, Harvard Medical School and Brigham & Women's Hospital, Boston, Massachusetts 02215

²Functional Molecular Imaging Center, Brigham and Women's Hospital, Massachusetts 02115

³Department of Cell Biology and the CBR Institute of Biomedical Research, Harvard Medical School, Boston, Massachusetts 02115

Received 29 January 2007; Revision Received 16 March 2007; Accepted 22 March 2007

Grant sponsor: Center for Bioinformatics Research Program grant (Harvard Center of Neurodegeneration and Repair); Grant sponsor: NIH/NLM; Grant number: R01 LM008696.

*Correspondence to: Prof. Xiaobo Zhou, Functional Molecular Imaging Center, Brigham and Women's Hospital, MA 02115, USA.

Email: zhou@crystal.harvard.edu

Published online 31 May 2007 in Wiley InterScience (www.interscience.wiley.com)

DOI: 10.1002/cyto.a.20411

© 2007 International Society for Analytical Cytology

• Abstract

Recent development of detection techniques of molecular particles in live cells has stimulated interest in developing the new powerful techniques to track the molecular particles in live cells. One special type of cellular microscopy images is about the formation and transportation of clathrin-coated pits and vesicles. Clathrin-coated pits are very important in studying the behavior of proteins and lipids in live cells. To answer the question, whether there exist "hot spots" for the formation of Clathrin-coated pits or the pits and arrays formed randomly on the plasma membrane, it is necessary to track many hundreds of individual pits dynamically in live-cell microscope movies to capture and monitor how pits and vesicles were formed. Therefore, a motion correspondence algorithm based on fuzzy rule-based system is proposed to resolve the problem of ambiguous association encountered in these dynamic, live-cell images of clathrin assemblies. Results show that this method can accurately track most of the particles in the high volume images. © 2007 International Society for Analytical Cytology

• Key terms

clathrin-coated pits; particle tracking; motion correspondence; fuzzy rule-based system

RECENTLY, biologists find that Clathrin-coated pits and vesicles are very important for proteins and lipids to be removed from the plasma membrane (endocytosis) and transported to an internal compartment (endosome) (1–13). Clathrin-coated pits and vesicles can be found in all nucleated cells, from yeast to humans, as shown in Figures 1 and 2. It is meaningful to build up automatic tracking algorithm to analyze the mechanism of the formation and transportation of clathrin-coated pits which is discussed in Refs. 4–6 and 14. However, significant challenges exist in the detection of all the particles correctly in the live-cell movie, because of the noisy background and the low contrast in those movies (Figs. 1 and 2).

To solve the tracking problem, we need to deal with the detection problem first. Lately, a novel method has been proposed to detect the molecular particles in live cell (14). In Ref. 14, the authors introduce Haar features which combined the intensity information and the shape information of the particles to overcome the problem from the noisy background and the low contrast. Since the quantity of Haar features is too large, a machine learning method which includes the Adaboost algorithm and "Cascade" idea is used to increase the computation speed. Therefore, this method has the potential to provide a cost-effective solution to resolve detection of subcellular molecular particles in living cells. Experimental results show that this machine learning algorithm based on Haar features can detect most of the particles and extract the boundaries of the particles accurately. Then we can extract the features for tracking algorithm, such as the centroid of the particles and the shape and intensity information, using the novel detection method.

Computerized analysis of cellular microscopy images is dependent upon the development and the integration of automated segmentation, tracking, and feature extraction for this new class of image data types. The general framework of analysis

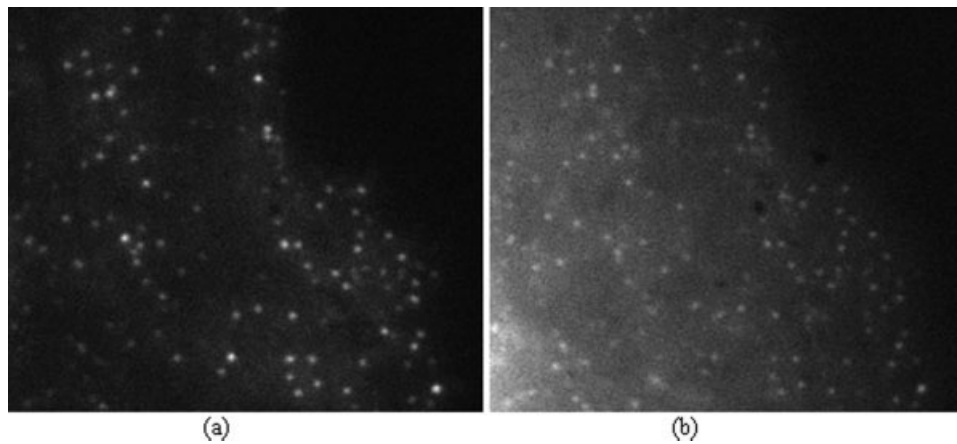


Figure 1. The tenth frame of Tirf (a) and Epi (b) data.

in molecular dynamics studies is summarized in Figure 3. For the detection part, we adopt the detection method proposed in Ref. 14. In this article, we focus on building the algorithm to track many hundreds of individual pits as they form, by visualizing clathrin light chain, and track whether the pit is successful in forming a vesicle, by simultaneously visualizing the cargo.

Scientists can now track single particles automatically (3), by using five algorithms stated in the review paper (15): the centroid method, the Gaussian fit method, the correlation method, the sum-absolute difference method, and the interpolation method. These methods cannot be simply applied to our biological problem; however, as single-particle tracking lacks the ambiguous association caused by the touching spots of particles in multiparticle tracking. Model based tracking method (16) and shape based tracking method are also developed, but they cannot solve the correspondence problem. Recently, many algorithms have been developed trying to solve the correspondence problem in the motion of particles and cells (17–21). One method is based on appearance features

(20), it assumes that the shape of a certain cell or particle only changes slightly between consecutive frames. Another method is to maximize the smoothness of trajectory and the velocity of the particles (17,18) for the trajectory direction and the velocity of a moving particle only change slightly between consecutive frames. All these methods do not work well in our movies as only partial information of the particles' movement is considered.

The article concerns resolving the tracking problem described above, also shown in Figure 3. The major contribution of this article is to propose a motion correspondence method based on fuzzy logic which combines the smoothness features of the trajectory of the particles and the appearance features to deal with the ambiguous association problem in particles tracking.

In the next section, we introduce the materials and the detection method we adopted. In Particle Tracking Using Fuzzy Rule-based System, we introduce the automated tracking method based on fuzzy rule-based system. The results of the study are presented in Experimental Results. Finally, the

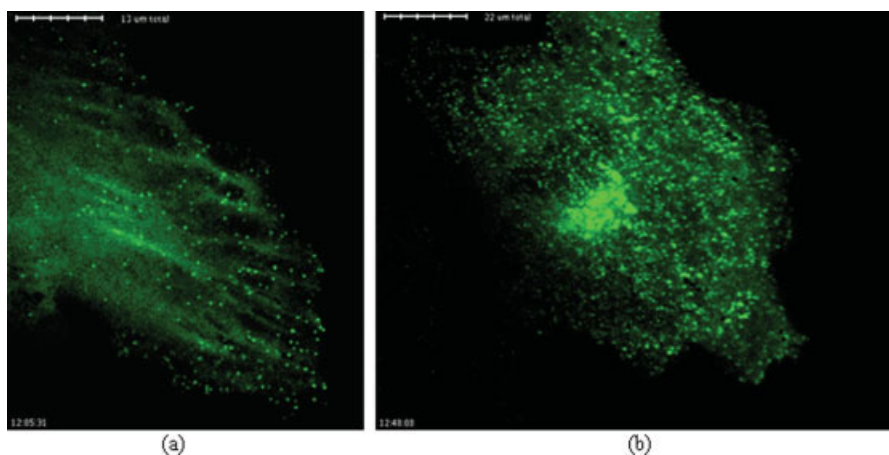


Figure 2. The tenth frame of Adaptor (a) and Clathrin (b) data.

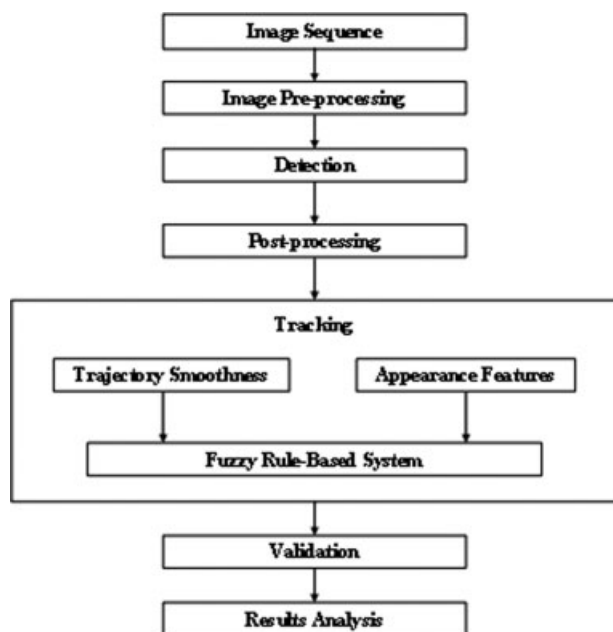


Figure 3. General description of our tracking system.

last two sections provide the Discussion and Conclusion of this article.

MATERIALS AND DETECTION

Four movies about the formation and transportation of clathrin-coated pits are studied in this article, i.e. the Total Internal Reflection Fluorescence (TIRF) movie, EPI (fluorescence microscopy) movie, Adaptor movie, and Clathrin movie. Some frames of these movies are selected to show in Figures 1 and 2. For the details of the material, we refer to the Part I (14). To analyze the statistical properties of the dwelling time distributions of clathrin-coated pits and vesicles inside a cell, we have to track the movement of all the particles accurately. However, the particle tracking in large scale has not been studied yet systematically in literature because ambiguous correspondence is a challenging problem.

The performance of automatic tracking algorithm strongly depends on the detection results. Since it is mentioned in Ref. 14 that many current detection methods are failed to detect the particles accurately, we adopt the novel method via machine learning proposed in Ref. 14. First, we need to create the big “sample pool” which includes 2,000 positive samples and 10,000 negative samples. Second, we use the Adaboost algorithm to select a small number of critical visual features from a larger set of features to yield a cost-effective classifier. Third, “Cascade” method is used to increase the computation speed. After we get the classifier, we need to do the validation and test. All of the results show that this method can reach a high accuracy (more than 95%) in detection. Some features that we are interested in are extracted

from the segmentation of particles, such as centroid position, shape, and intensity.

PARTICLE TRACKING USING FUZZY RULE-BASED SYSTEM

After particles are detected in all relevant frames, particles can be tracked by motion correspondence algorithm. The development and challenges in automated tracking and analysis of moving objects in image sequences are reviewed in Ref. 22. If small particles are moving individually and independently, many single-particle tracking methods can be used (3,15,23). However, there are several situations where those methods are not applicable. For example, particles may approach one another at distances that can no longer be distinguished so that they merge into one single spot. Or in reverse, a large spot that seems to be a single particle in one slice may split into several small particles in the next slice. The main goal of our tracking method is to solve the ambiguous correspondence problem in particles movement.

Since biologists are merely interested in particles that are 2 or 3 pixels in diameter, a consensus on the shape and contour of the particles with images of strong background noise and low contrast is never reached. Therefore, when several spots are moving very close, it is difficult to determine which spot is the right child spot in the next frame only depending on the appearance features. Furthermore, it would link the wrong correspondence particle by the deterministic method at most time. Another problem we encountered is to define the number of particles in one large spot as the merging and splitting would occasionally occur simultaneously. Therefore, we design a fuzzy-logic system (19,24) combined with different parameters to tackle these problems. Fuzzy-logic system has been successfully applied to many areas (24) such as the area of auto control (25) and neural networks (24). Fuzzy logic controllers are successfully applied in back-driving a truck model (25). It can track the moving trajectory of the truck subject to certain path constraint. Fuzzy-logic system can also take advantage of an array of learning mechanisms primarily originating within the theory of neuron-computing and the use of the rule-based systems (24). These advantages of fuzzy-logic system are part of the reason that motivated us to develop our particle tracking system.

In our fuzzy-logic system, we use four parameters θ_1 , θ_2 , θ_3 , and θ_4 to describe the “similarity” of the particles between consecutive frames. In some cases, the nearest neighbor spot in the next frame is not the right spot corresponding to the current spot. Hence the pure distance measurement is not good enough for performing tracking. That motivates us to extend the definition of the “distance”. Let θ_1 and θ_2 denote the angle parameter and the velocity parameter (17,18), respectively. They are used to describe the smoothness of trajectory and the consistency of velocity of the moving particles between the three consecutive frames. The velocity parameter θ_2 is also known as the relative displacement of the center coordinate of the moving particles between the consecutive frames. θ_2 and θ_3 denote the difference of the total intensity and the area of the spots. They are used to describe the spatial proximity

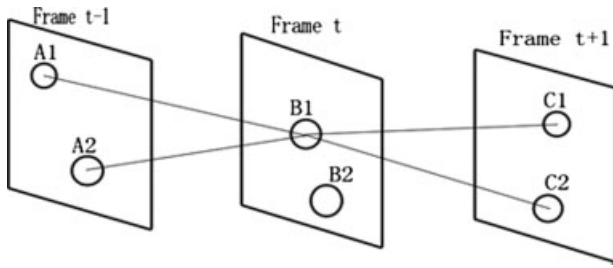


Figure 4. Motion of particles in 3D spatiotemporal space through consecutive frames. For particle B1 (x_{B1}, y_{B1}, t), the angle parameter θ_1 and the velocity parameter θ_2 are computed in each path and parameters θ_3 and θ_4 are computed between the candidate parent spots A1 (or A2) and current spot B1.

and the similarity of the spots in appearance between consecutive frames. The parameters θ_1 and θ_2 are computed by substantially maximizing the smoothness of trajectory and velocity of particles. The original algorithm in Refs. 17 and 18 only considers the positions of particles in a 2D space. However, intuitively the clathrin spots migrate in time-space and sometimes the particles move towards z -axis direction. In this case, the 2D algorithm is not able to find the maximum smoothness trajectory. Therefore, we consider the spatiotemporal information, i.e., the coordinate of particle B is (x_B, y_B, t) in the frame t and the parameters θ_1 and θ_2 are calculated for each trajectory of particles in 3D space, see in Figure 4. Here we consider three image frames taking at time $t - 1$, t , and $t + 1$. For each candidate parent spot A in frame $t - 1$ and child spot C in frame $t + 1$ for the current studying spot B in frame t , we calculate the angle parameter θ_1 and the velocity parameter θ_2 by

$$\theta_1 = -\frac{\|\overline{AB}\|^2 + \|\overline{BC}\|^2 - \|\overline{CA}\|^2}{2\|\overline{AB}\| \cdot \|\overline{BC}\|} \quad (1)$$

$$\theta_2 = \frac{2(\|\overline{AB}\| \cdot \|\overline{BC}\|)^{1/2}}{\|\overline{AB}\| + \|\overline{BC}\|} \quad (2)$$

Out of the convenience of computation, θ_3 and θ_4 are computed in normalization form,

$$\theta_3 = 1 - \left| \frac{I_t - I_{t-1}}{I_t + I_{t-1}} \right| \quad (3)$$

$$\theta_4 = 1 - \left| \frac{S_t - S_{t-1}}{S_t + S_{t-1}} \right| \quad (4)$$

where I_t is the total intensity of the spots in frame t , and S_t is the total area of the spots in frame t . Next, there are four features θ_{1A} , θ_{2A} , θ_{3A} , and θ_{4A} for each candidate parent particle A to estimate its similarity to the current spot B . Next we employ Fuzzy-logic system to estimate the similarity.

Fuzzy-logic system formulates the associative mapping from a given input in regards to a close output without requiring a mathematical description of the functional correlation between the input and the output. First, the fuzzy theory assumes that all things are a matter of degree (26). A fuzzy system redefines the classical concept of “set” to “fuzzy set” by choosing the appropriate membership function. The membership of an element is measured by a degree, commonly known as the “membership degree” of that element to the set, and it takes a value in the interval $[0, 1]$ by agreement. The fuzzy model is described by certain fuzzy *If-Then* rules. These fuzzy rules are based on certain linguistic labels H_1, \dots, H_5 . For example, H_1 and H_2 can be defined as “more-smooth,” “median-smooth,” and “less-smooth” for parameters θ_1 and θ_2 ; H_3 and H_4 can be defined as “little-difference” and “large-difference” for parameters θ_3 and θ_4 ; H_5 can be defined as “most-similar,” “median-similar,” and “least-similar” for the decision fuzzy set. The decision fuzzy set is based on the expression of the concept of “similarity” between the parent spot and the current spot. For the candidate parent spot, A_k , $k = 1, \dots, n$, where n is the total number of the candidate parent spot, we define the i th rule of the fuzzy model as follows:

Rule i : If θ_{1A_k} is H_{i1} and \dots and θ_{4A_k} is H_{i4} ,
then A_k is H_{i5} , $i = 1, 2, \dots, L$

In our fuzzy-logic system, we define five such production rules, i.e., $L = 5$. In each rule, the membership functions h_{i1}, \dots, h_{i4} are used to fuzzify the input variables $\theta_1, \dots, \theta_4$ based on the different linguistic labels H_{i1}, \dots, H_{i4} . According to each feature’s property, we use Gaussian function to fuzzify the parameters θ_1 and θ_2 and use trapezoid function to fuzzify the parameters θ_3 and θ_4 . That is,

$$h_{i1}(\theta_1; \mu, \sigma) = \exp\{-\frac{(\theta_1 - \mu)^2}{2\sigma^2}\}, \quad (5)$$

$$h_{i3}(\theta_3) = \begin{cases} 0, & x \leq 0.6 \\ (\theta_3 - 0.6)/0.2, & 0.6 < \theta_3 < 0.8 \\ 1, & 0.8 \leq x \leq 1 \end{cases} \quad (6)$$

where μ and σ are the mean and the standard deviation of the Gaussian distribution, for example, we choose $\mu = 0.1$ and $\sigma = 1$ to describe the linguistic label “more-smooth”. The Eq. (6) is chosen to describe the linguistic label “little-difference” and the “large-difference” is described as the same way by choosing the different parameters. We also use the triangular function (7) to create the decision fuzzy set based on linguistic label “most-similar.”

$$Q_i(x) = \begin{cases} 0, & x \leq 0.7 \\ (x - 0.7)/0.3, & 0.7 < x \leq 1 \end{cases}, \quad x \in [0, 1]. \quad (7)$$

The above *If-Then* fuzzy rules can be then formulated as the following system:

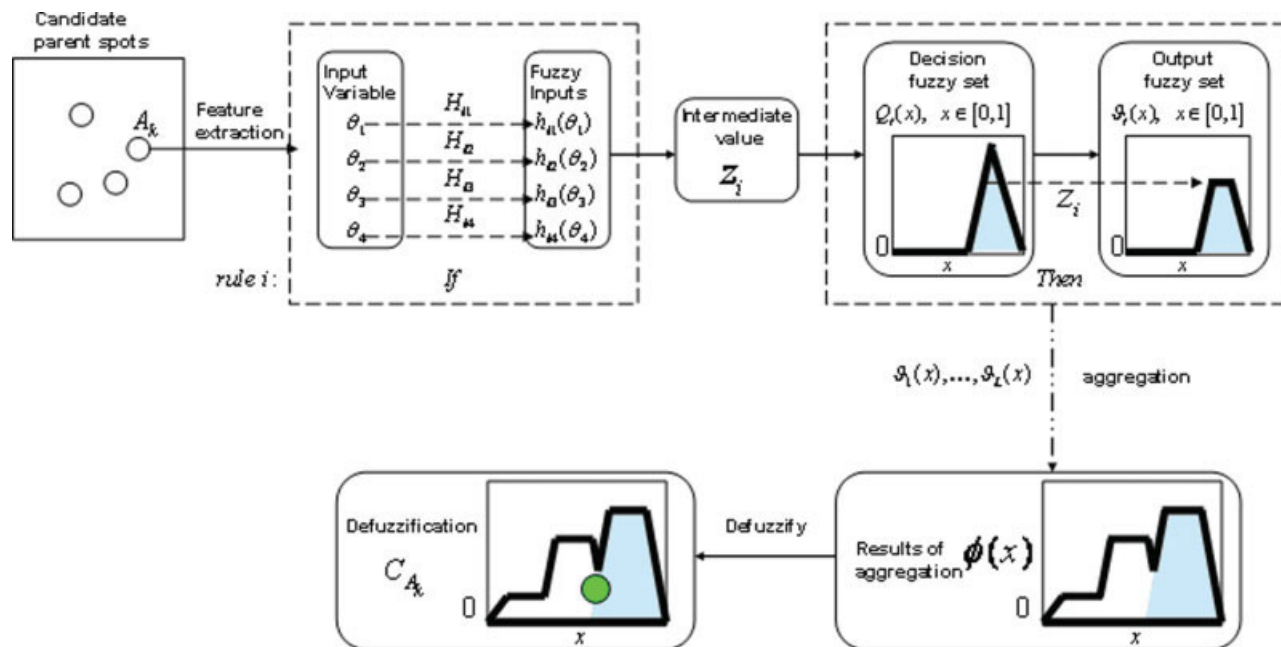


Figure 5. The flow chart of a fuzzy rule-based system. [Color figure can be viewed in the online issue, which is available at www.interscience.wiley.com.]

$$z_i = \max\{h_{i1}(\theta_1), \dots, h_{i4}(\theta_4)\}$$

$$\vartheta_i(x) = \begin{cases} Q_i(x) & Q_i(x) \leq z_i \\ z_i & Q_i(x) > z_i \end{cases} \quad x \in [0, 1] \quad \text{for } i = 1, 2, \dots, L \quad (8)$$

where $\theta_1, \dots, \theta_4$ are the input variables and z_i is the intermediate result which maximizes the fuzzy input variables because we want to get the “most similar” result. $\vartheta_i(x), x \in [0, 1]$ is the output fuzzy set to the candidate parent spot, $A_k, k = 1, \dots, n$, under the rule i . The process of the fuzzy rule-based system is shown in Figure 5. First, several candidate parent spots (A_1, \dots, A_n) are determined in frame $t - 1$ for the current spot in frame t . For each candidate parent spot, $A_k, k = 1, \dots, n$, four parameters $\theta_{1A_k}, \dots, \theta_{4A_k}$ are extracted as the input variables to the fuzzy rule-based system. The intermediate result z_i is the maximum of all the fuzzy input variables $h_{i1}(\theta_1), \dots, h_{i4}(\theta_4)$. We use the intermediate result, z_i , to reshape the decision fuzzy set $Q_i(x)$ and then get the output fuzzy set ϑ_i of the system under the i th fuzzy rule. After we get all the output fuzzy set based on different fuzzy rules, we can use another fuzzy operator \max to aggregate them into one fuzzy set,

$$\phi(x) = \max\{w_1\vartheta_1(x), \dots, w_L\vartheta_L(x)\}, \quad x \in [0, 1] \quad (9)$$

where w_i is the weight that is assigned to the different rules and $L = 5$. In our system, we choose the weight as (1, 1, 0.8, 0.2, 0.5). Because of the assistance of the fuzziness of the input variables to the evaluation of the rule during the intermediate

steps, the final desired output for each candidate parent spot is generally a single number. Therefore, we aggregate all the fuzzy outputs based on the rules to a single fuzzy decision value for comparison later. This procedure is called “defuzzification”. In this study, we use the most popular defuzzification method—the centroid calculation,

$$C_{A_k} = \frac{1}{M} \int_0^1 \phi(x)x dx \quad (10)$$

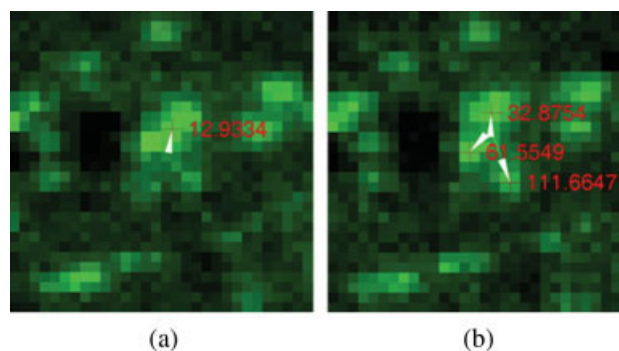


Figure 6. Large spot splits into three small spots. Small region extracted from the consecutive frames and enlarged twenty times. (a) The spot has been tracked before splitting; (b) The spot is splitting into three small spots. White arrow means the movement direction of spots, the red crosses are the detection centers of the spots and the red numbers beside the cross are the spots’ velocities (nm/s). [Color figure can be viewed in the online issue, which is available at www.interscience.wiley.com.]

Table 1. Comparison of automatic and manual tracking

MOVIE	POSITION ERRORS (PIXELS)		TRACKED PARTICLES (%)
	AUTOMATIC		
	AVG.	RMSE	AUTOMATIC
TIRF	0.2941	0.1701	95.28
EPI	0.4491	0.2651	95.48
Adaptor	0.3180	0.1800	95.32
Clathrin	0.3740	0.2579	94.37
Average	0.3588	0.2183	95.11

Tabulated values are the average (AVG.) and root mean square error (RMSE) of position errors and percentage of the tracked particles from automatic tracking compared to manual tracking. The last row indicates average over all four movies. All values are in pixels.

where M is the total area (or total mass) of the output fuzzy system; $\phi(x)$ is the membership degree of the member $x \in [0,1]$. C_{A_k} , also called the center of gravity, is the center of fuzzy system ϕ and it represents the similarity between the particle and its parent candidate A_k —the high value of C_{A_k} represents the high similarity. In the tracking process, we calculate the similarity of the fuzziness, $\{C_{A_1}, \dots, C_{A_n}\}$, to find the most ‘similar’ corresponding object $A_{\hat{k}}$,

$$\hat{k} = \arg \max_{k \in \{1, \dots, n\}} \{C_{A_k}\}. \tag{11}$$

If no corresponding spot is found in the previous image slice, it symbolizes that there was no parent particle. This spot will be set to a new trajectory and be defined as the new starting point. If no corresponding spot is found in the next slice, it symbolizes that there was no child particle. The corresponding spot will be set to the last object of the respective track, and this track will be terminated. For the merging case, the child spot chooses the ‘most similar’ spot of the parent. That means the most likely parent spot devours other spots to a big one. After the merging process, the former spots could not be detected by any other method because the particle lacks a distinct shape and contour. So we stop the trajectory of the vanished spots and record the orientation of their movements. For the splitting case, since all child spots can accurately find their true parent spots, only trajectory is needed, see Figure 6.

EXPERIMENTATION RESULTS

We studied four movies shown in Figures 1 and 2 to show that the proposed approach is effective for automatic particle tracking. Two of the movies, Adaptor and Clathrin discussed in Ref. 2, are available in the corresponding Cell

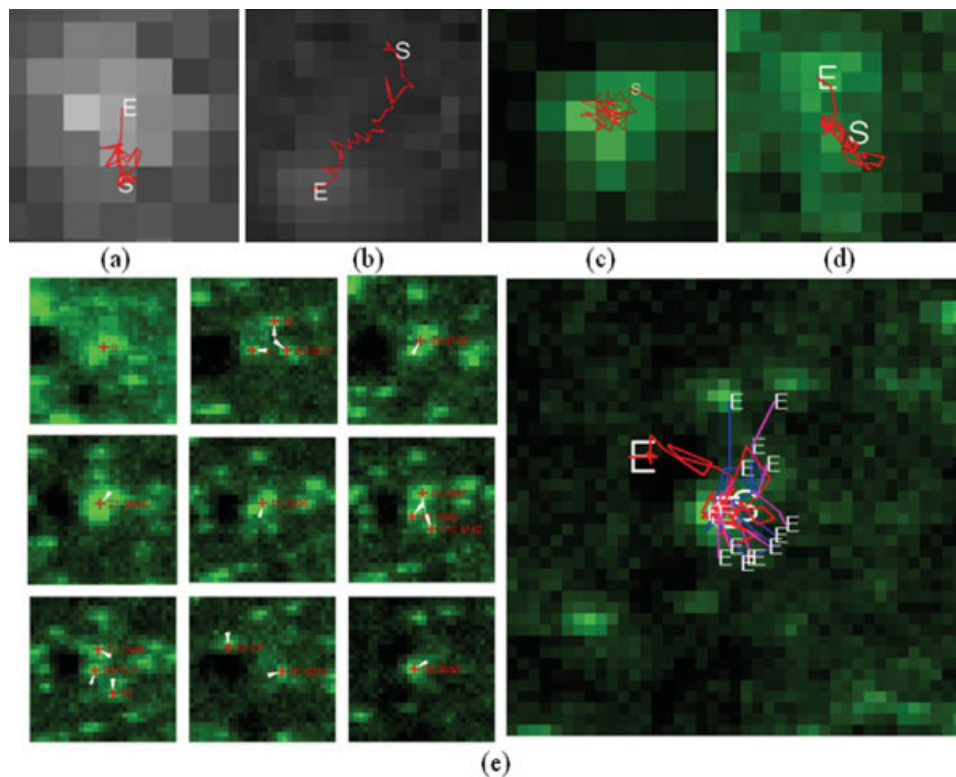


Figure 7. Detection and tracking of motile spots of TIRF, EPI, Adaptor, and Clathrin movies. S indicates the start point of the trajectory while E indicates the end point of the trajectory. Positions of spots in the displayed frame are marked with “+”. (a–d) Four single spot trajectories chosen from TIRF, EPI, Adaptor, and Clathrin movies. (e) An active spot split and merge several times during its “living”; nine small images on the left are taken at time periods 1, 10, 12, 28, 38, 39, 40, 50, and 78; the final picture shows its trajectory including the small split spots. Big “E” means the end point of the major trajectory of this spot, and small “E” indicates the end point of the short life split spots. [Color figure can be viewed in the online issue, which is available at www.interscience.wiley.com.]

website. The details of the material are discussed in the Part I (14). In this section, we discuss the accuracy of particle tracking. The proposed methods are implemented in Matlab.

For spot tracking, validation is very challenging because many particles vanish or appear in the field of view. To establish a metric for the performance of the tracking algorithm, two types of errors are considered.

- Percentage of the tracked particles. Since it is difficult (actually almost impossible) to count the tracked particles for the whole video timing period, our trial data consist of 50 image sequences. The tracking performance is defined as the number of cells tracked without termination divided by the total number of target particles.
- Root mean square error (RMSE) of the tracked particle center positions. The RMSE is computed over all frames in a tracking video sequence. Manually determined particle positions are used to compute the position error.

Our trial data consist of four different movies, TIRF, EPI, Adaptor, and Clathrin shown in Figures 1 and 2. The comparison between automatic and manual tracking validation results is shown in Table 1. For the manually-obtained trajectories, first we need to label the center of the particle manually in different frames and then we link all these center positions of the particle during it is “alive” in the movie. It is difficult to find the accurate centers of the spots, because most spots are just a few pixels in size. However, the averages of the position errors are just between 0.29 and 0.45, and the RMSE of the position errors are between 0.17 and 0.27. The percentages of the tracked particles are between 94.37 and 95.48%, and the average percentage of the tracked particles of all four movies is 95.11%.

Some spots’ trajectories in Figure 7 show our algorithm is efficient to these movies. We have also chosen several single spots to compare the manual measurements of their velocities with the measurements generated by the automatic algorithm.

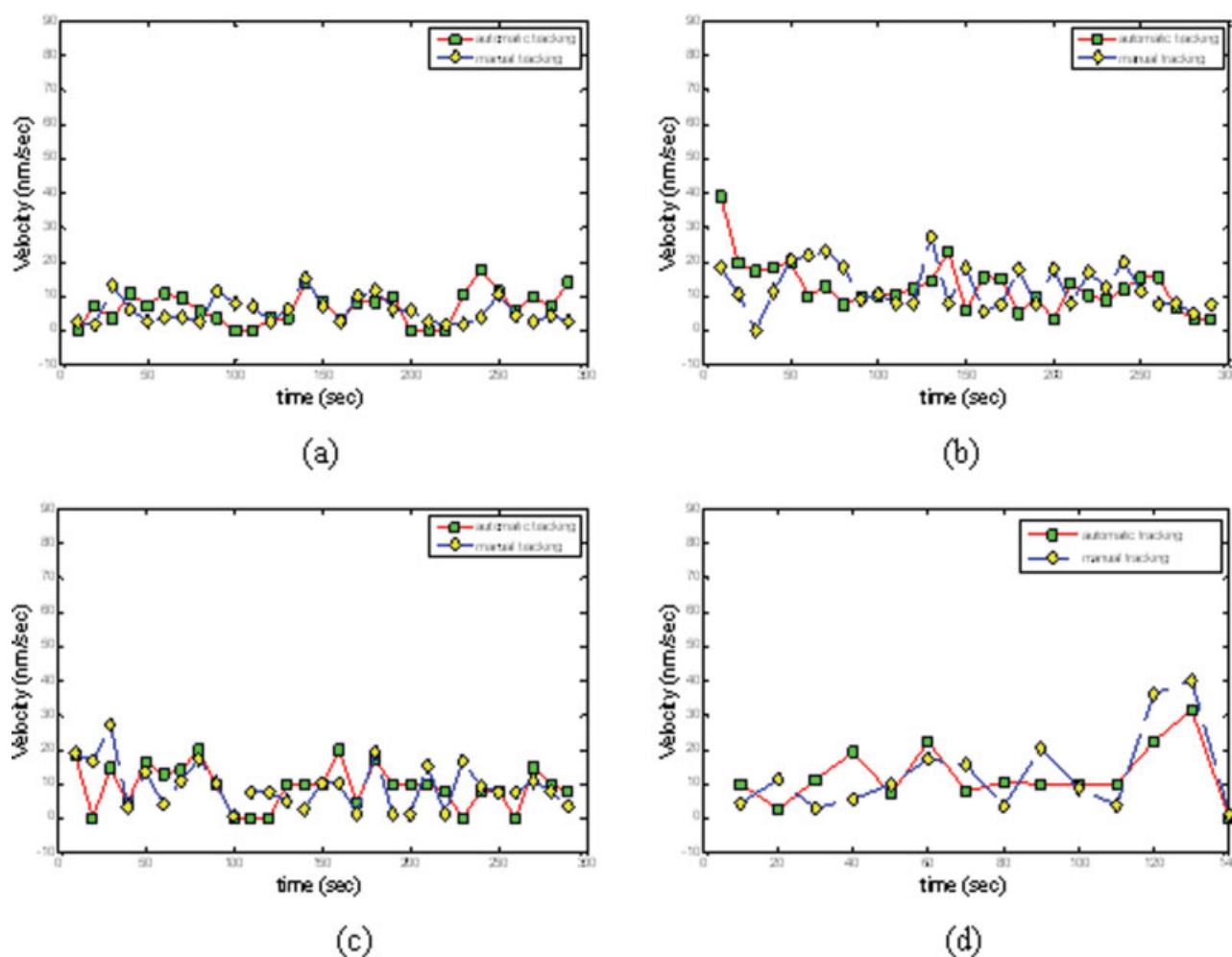


Figure 8. Four instances of manual versus automatic extracted measurements of a single particle velocity from different movies. (a-d) are the velocity comparisons for the TIRF, EPI, Adaptor, and Clathrin movies. [Color figure can be viewed in the online issue, which is available at www.interscience.wiley.com.]

Results are shown in Figure 8. From these results, the automatic tracking can be considered to be at least as accurate, if not more accurate, than manual tracking.

DISCUSSION

In fuzzy rule-based system, we need to pay more attention to the parameter selection and fuzzy rule selection. For parameter selection, if the inappropriate parameters are selected, the consequent model will fail to fit the requirement of tracking the particles which we want to analyze. Four parameters, such as differences in velocity, deviation of expected extrapolated position from the potential new position and differences in total intensity and area, are used in Ref. 19. However, in our data, the deviation of expected extrapolated position is hard to calculate because the different properties are in the different stages of the formation and transportation of clathrin coated pits which is discussed in Part I (14). For example, coat propagation in the stage 2, we know that the particles stay at the same place to complete this process, while in the transportation stage, there are three different types about the clathrin coated pits (refer to Fig. 1 of Part I (14)). Since we want to monitor the whole process of the formation and transportation of clathrin coated pits, the expected extrapolated position is impossible and inappropriate in tracking the particles. To deal with the complex case that the particles merge and split frequently, we introduce additional parameters in our method, i.e. the angel parameter and the velocity parameter. For fuzzy rule selection, it also plays an important role in fuzzy rule-based system, and it strongly affects the performance of the whole tracking algorithm. Each fuzzy rule connects one parameter and the corresponding model, so we need to choose the right model to describe the property of the movement and behavior of the particles within a cell. In our program, we use the trapezoid function to describe the change of total intensity and area. If the change is small, then the weighted value is large. The constants, 0.6 and 0.8, are determined by experiments to distinguish the difference between “large-difference” and “little-difference.”

Next, we compare our proposed method with the centroid based tracking method in Ref. 15 and the fuzzy rule-based method presented in Ref. 19. The centroid based tracking method is quite simple for only comparing the centroid position between the two consecutive frames. So, the centroid based tracking method can only track the individual trace and it is unstable to the different distance restriction. Figures 9a and 9b show the results of centroid based tracking method. If we set the different restrictions that displacement must be smaller than 3 or 10, we can get the totally different results shown in Figures 9a and 9b. We apply the fuzzy rule-based method presented in Ref. 19 after removing the parameter-deviation of expected extrapolated position and the result is shown in Figure 9c. It is easy to find out that our improved fuzzy rule-based method is much better than the other two methods from Figure 9.

Another justification is about the quantity of trajectories. For TIRF data, we get 1,927 traces in total and 972 traces (the particles' life is larger than 3) within 150 frames from the

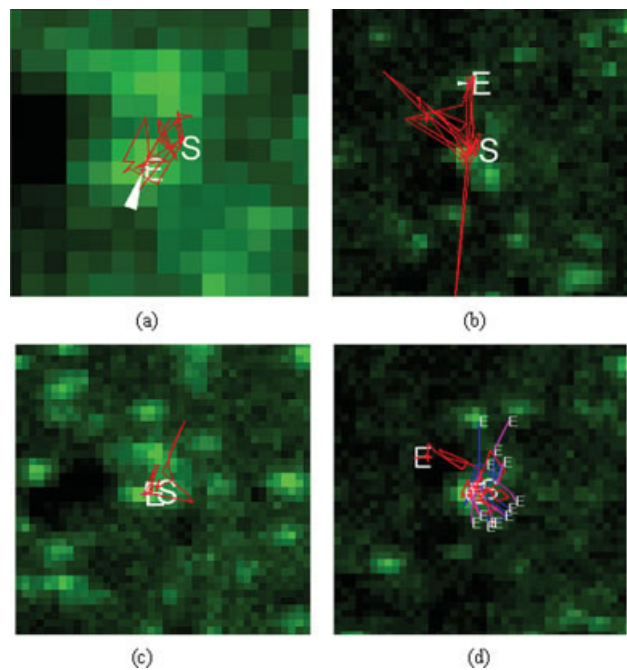


Figure 9. Comparison of the centroid based tracking method, fuzzy rule-based method and corrected fuzzy rule-based method. (a) is the result of centroid based tracking method with the displacement restriction 3. (b) is the result of centroid based tracking method with the displacement restriction 10. (c) is the result of fuzzy rule-based method presented in Ref. 21. (d) is the result of the improved fuzzy rule-based method we proposed. [Color figure can be viewed in the online issue, which is available at www.interscience.wiley.com.]

improved fuzzy rule-based method, while we get 3,140 traces in total and 730 traces for the particles whose life is larger than 3 using the fuzzy rule-based method presented in Ref. 19. It gives us a justification that in some case the method in Ref. 19 could not track the whole formation and transportation of clathrin-coated pits and separates one trace which we assume it is a real trace into several short traces because the method in Ref. 19 is not designed for solving ambiguous correspondence and it considers fewer information of the movement of the particles than our method does. However, we deal with the tracking of all the clathrin-coated pits, including the touching spots. We obtain the similar results for our other data.

However, there is limitation derived from the parameters selection. That is we cannot put much parameters in the fuzzy rule-based system, because the complexity of the system will exponentially increase and the whole system will be hard to interpret (27,28). Therefore, the redundant variables and rules are removed according to our understanding of the data. In the proposed fuzzy logic rule-based tracking method, we use four parameters θ_{1A} , θ_{2A} , θ_{3A} , and θ_{4A} to describe the “similarity” of the particles between consecutive frames. To our best knowledge, these four parameters are the prior information we can use to describe the movement of the particles so far.

CONCLUSION

To simultaneously track multiple particles in the dynamic images of living cells with strong background noise and low contrast, the traditional tracking methods such as single-particle tracking or tracking methods based on spatial property, do not work. In this study, a method developed by combining trajectory smoothness method with fuzzy rule-based system was proposed to deal with the problem of ambiguous association encountered in these dynamic, live-cell images of clathrin assemblies. Results show that the proposed method worked well for representative movies with the tracking of clathrin coated pits, vessels, and receptors. The method presented here thus has the potential to provide a cost-effective solution to resolve tracking of subcellular molecular particles in living cells.

The next step of this research will focus more on biostatistics analysis. For example, we can go in the deep study of the distribution of the dwell time, size, and intensity change of Clathrin-coated pits and vesicles inside a cell. We also can study the spatial distribution of the Clathrin-coated pits and vesicles by using K function (29), Quadrat method (30), Mantel matrix randomization test (30), nearest neighbor methods (31), and Markov chain Monte Carlo method.

ACKNOWLEDGMENTS

The authors would like to acknowledge the collaboration with their biology collaborators in the Department of Cell Biology and The CBR Institute of Biomedical Research at Harvard Medical School in this research effort. They would like to thank other research members of the Life Science Imaging Group of the HCNR Center for Bioinformatics, Brigham and Women's Hospital, Harvard Medical School for their technical comments.

LITERATURE CITED

- Gaidarov I, Santini F, Warren RA, Keen JH. Spatial control of coated-pit dynamics in living cells. *Nat Cell Biol* 1999;1:1–7.
- Ehrlich M, Boll W, Oijen AV, Hariharan R, Chandran K, Nibert ML, Kirchhausen T. Endocytosis by random initiation and stabilization of clathrin-coated pits. *Cell* 2004;118:591–605.
- Ghosh RN, Webb WW. Automated detection and tracking of individual and clustered cell surface low density lipoprotein receptor molecules. *J Biophys* 1994;66:1301–1318.
- Hirst J, Robinson MS. Clathrin and adaptors. *Biochim Biophys Acta Mol Cell Res* 1998;1404:173–193.
- Kirchhausen T. Clathrin. *Ann Rev Biochem* 2000;69:699–727.
- Kirchhausen T. Three ways to make a vesicle. *Nat Rev Mol Cell Biol* 2000;1:187–198.
- Kirchhausen T. Clathrin adaptors really adapt. *Cell* 2002;109:413–416.
- Merrifield CJ, Feldman ME, Wan L, Almers W. Imaging actin and dynamin recruitment during invagination of single clathrin-coated pits. *Nat Cell Biol* 2002;4:691–698.
- Puertollano R, Wel NNvd, Greene LE, Eisenberg E, Peters PJ, Bonifacino JS. Morphology and dynamics of clathrin/GGA1-coated carriers budding from the trans-Golgi network. *Mol Biol Cell* 2003;14:1545–1557.
- Rappoport JZ, Simon SM. Real-time analysis of clathrin-mediated endocytosis during cell migration. *J Cell Sci* 2003;116:847–855.
- Rappoport JZ, Taha BW, Simon SM. Movement of plasma-membrane-associated clathrin spots along the microtubule cytoskeleton. *Traffic* 2003;4:460–467.
- Won CS. *Stochastic Image Processing*. New York: Kluwer Academic/Plenum; 2004.
- Zhou X, Wang X. FIR-Median hybrid filters with polynomial fitting. *J Digital Signal Process* 2004;14:112–124.
- Jiang S, Zhou XB, Kirchhausen T, Wong STC. Detection of molecular particles in live cells via machine learning. *Cytometry A* 2007;71A, in press. doi://10.1002/cyto.a.20404.
- Cheezum MK, Walker WF, Guilford WH. Quantitative comparison of algorithms for tracking single fluorescent particles. *Biophys J* 2001;81:2378–2388.
- Debeir O, Camby I, Kiss R, Van Ham P, Decaestecker C. A model-based approach for automated in vitro cell tracking and chemotaxis analyses. *Cytometry A* 2004;60A:29–40.
- Eden E, Waisman D, Rudzsky M, Bitterman H, Brod V, Rivlin E. An automated method for analysis of flow characteristics of circulating particles from in vivo video microscopy. *IEEE Trans Med Imaging* 2005;24:1011–1024.
- Chetverikov D. Particle image velocimetry by feature tracking. *Comput Anal Images Patterns* 2001;2124:325–332.
- Tvaruskó W, Bentele M, Misteli T, Rudolf R, Kaether C, Spector DL, Gerdes HH, Eils R. Time-resolved analysis and visualization of dynamic processes in living cells. *Proc Natl Acad Sci USA* 1999;96: 7950–7955.
- Egmont-Petersen M, Shreiner U, Tromp SC, Lehmann TM, Slaaf DW, Arts T. Detection of leukocytes in contact with the vessel wall from in vivo microscope recordings using a neural network. *IEEE Trans Med Imaging* 2000;47:941–951.
- Saban M, Altinok A, Peck A, Kenney C, Feinstein S, Wilson L, Rose K, Manjunath BS. Automated tracking and modeling of microtubule dynamics. *Proc IEEE Int Symp Biomed Imaging* 2006;1032–1035.
- Meijering E, Smal I, Danuser G. Tracking in molecular bioimaging. *IEEE Signal Process Mag* 2006;23:46–53.
- Ewers H, Smith AE, Sbalzarini IF, Lilie H, Koumoutsakos P, Helenius A. Single-particle tracking of murine polyoma virus-like particles on live cells and artificial membranes. *Proc Natl Acad Sci USA* 2005;102:15110–15115.
- Pedrycz W. Heterogeneous fuzzy logic networks: Fundamentals and development studies. *IEEE Trans Neural Networks* 2004;15:1466–1481.
- Liu Z, Li HX. A probabilistic fuzzy logic system for modeling and control. *IEEE Trans Fuzzy Systems* 2005;13:848–859.
- Mendel JM. *Introduction to Rule-Based Fuzzy Logic Systems*. Piscataway, NJ: IEEE; 2001.
- Yaochu Jin. Fuzzy modeling of high-dimensional systems: complexity reduction and interpretability improvement. *IEEE Trans Fuzzy Syst* 2000;8:212–221.
- Passino KM, Yurkovich S. *Fuzzy Control*. Menlo Park, CA: Addison Wesley Longman; 1998.
- Ripley BD. The second-order analysis of stationary point processes. *J Appl Probab* 1976;13:255–266.
- Ripley BD. *Spatial Statistics*. New York: Wiley; 1981.
- Cressie N. *Statistics for Spatial Data*. New York: Wiley; 1993.